Journal Name

ARTICLE

Heteroatom Substitution Effects in Spin Crossover Dinuclear Complexes

Received 00th January 20xx,
Accepted 00th January 20xx

DOI: 10.1039/x0xx00000x

www.rsc.org/

Samantha Zaiter,[a] Charlotte Kirk,[b] Matthew Taylor,[c] Y. Maximilian Klein,[d] Catherine E. Housecroft,[d] Natasha F. Sciortino,[a] John E. Clements,[a] Richard I. Cooper,[b] Cameron J. Kepert[a] and Suzanne M. Neville*[c]

We probe the effect of heteroatom substitution on the spin crossover (SCO) properties of dinuclear materials of the type $[Fe_2(NCX)_4(R\text{-}trz)_5]\cdot S$ (X = S, Se; S = solvent; R-trz = (E)-N-(furan-2-ylmethylene)-4H-1,2,4-triazol-4-amine (furtrz); (E)-*N*-(thiophen-2-ylmethylene)-4*H*-1,2,4-triazole-4-amine (thtrz)). For the furtrz family ($[Fe_2(NCX)_4(furtrz)_5]\cdot furtrz\cdot MeOH$; X = S (**furtrz-S**) and X = Se (**furtrz-Se**)) gradual and incomplete one-step SCO transitions are observed (**furtrz-S** ($T_{½}$ = 172 K) and **furtrz-Se** ($T_{½}$ = 205 K)) and a structural evolution from [HS-HS] to [HS-LS] per dinuclear species. Contrasting this, within the thtrz family ($[Fe_2(NCX)_4(thtrz)_5]\cdot 4MeOH$; X = S (**thtrz-S**) and X = Se (**thtrz-Se**)) more varied SCO transitions are observed, with **thtrz-S** being SCO-inactive (high spin) and **thtrz-Se** showing a rare complete two-step SCO transition ($T_{½\{1,2\}}$ = 170, 200 K) in which the Fe^{II} sites transition from [HS-HS] to [HS-LS] to [LS-LS] per dinuclear unit with no long range ordering of spin-states at the intermediate plateau. Detailed structure-function analyses have been conducted within this growing dinuclear family to rationalise these diverse spin-switching properties.

Introduction

The spin crossover (SCO) phenomenon, where high spin (HS) and low spin (LS) electronic configurations of certain d^4-d^7 transition metal ion complexes can be interconverted upon external energy input (i.e., temperature, pressure, light-irradiation), is a prime example of molecular switching.[1] In the solid state, spin-state transition character is derived collectively from a combination of inner (i.e., coordination bonds) and outer (i.e., supramolecular interactions) coordination sphere effects.[2] The strength and directionality of such bonds and interactions act to propagate the spin-state change throughout the solid, whereby effective pathways result in abrupt transitions, and define a direct or step-wise HS to LS transition of elastic origin.[3] Over the past few decades there have been numerous structural platforms devised from which to study and ultimately tune SCO properties through 'crystal engineering'. Of these, polynuclear SCO species provide many unique attractive features, notably providing both strong solid-state communication through direct coordination linkages and readily tailored, weaker supramolecular interactions (comprised of both host…host and host…guest interactions).[4]

Dinuclear complexes are an important subclass of polynuclear SCO species as they represent the most basic prototype of coordinatively bridged SCO metal ions.[5] The rational synthesis of dinuclear SCO species has been approached in several ways, affording two general structural classes: (1) those where the SCO sites are bridged by long organic linkers; and (2) those connected by short linkers (i.e., connected *via* only 2-3 atoms).[5] Irrespective of bridge length, from a structure-property perspective dinuclear species examples provide important fundamental insight into spin-state communication and cooperativity in polynuclear species. Along this line, one particularly important facet of dinuclear complex SCO behaviour is the array of spin-state progression pathways available within each dinuclear unit. More explicitly, within each dinuclear moiety (i.e., [Fe1-Fe2]) the SCO ions may undergo a direct HS to LS transition (i.e., [HS-HS] ↔ [LS-LS]), a 'half' transition (i.e., [HS-HS] ↔ [LS-HS]) with the 'mixed' spin-state species persisting until low temperature, or a complete stepwise transition (i.e., [HS-HS] ↔ [LS-HS] ↔ [LS-LS]). Other situations are also possible, such as pairs of co-existing [HS-HS] and [LS-LS] species,[6] but are less common. From a structural design perspective, the presence of 'mixed' spin state dinuclear species, [HS-LS], requires a structure that can accommodate distortion across the Fe-Fe bridge due to the substantial volumetric disparity between HS and LS state metal ions. Indeed, various reports[5,7] show that the strain caused by inherent distortion can result in trapped [HS-LS] species. In the related area of coordination polymer SCO materials, it has been shown[7] that such elastic strain ('frustration') across coordination bridges is a key factor for inducing multistep SCO

[a] School of Chemistry, The University of Sydney, New South Wales, 2006, Australia.
[b] Chemical Crystallography, Chemistry Research Laboratory, Mansfield Road, Oxford, UK.
[c] School of Chemistry, UNSW Sydney, New South Wales, 2052, Australia. s.neville@unsw.edu.au
[d] Department of Chemistry, University of Basel, BPR 1096, Mattenstrasse 24a, CH-4058, Switzerland

Electronic Supplementary Information (ESI) available: Further structural information available. See DOI: 10.1039/x0xx00000x

transitions and stabilising the energetically unfavourable existence of mixed spin-state species.

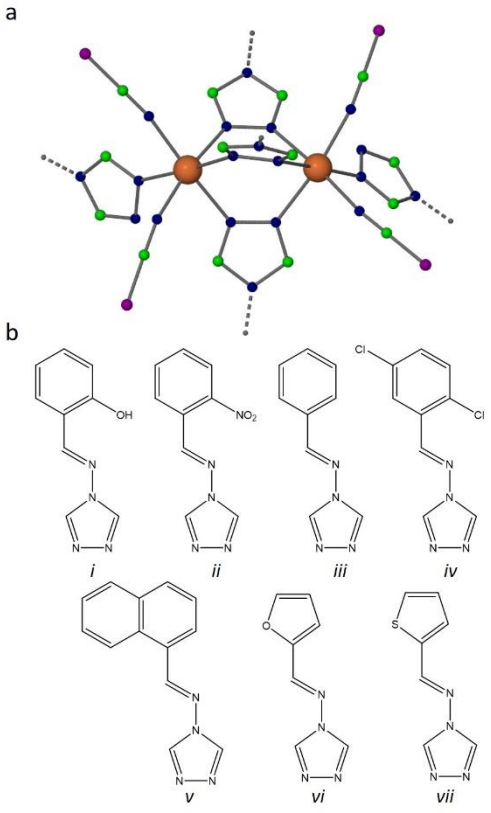

Figure 1. (a) The general core structure of $[Fe_2(R\text{-}trz)_5(NCX)_4]\cdot$(guest) (X = S, Se; Fe^{II} (orange), N (blue), C (green), X (purple)). (b) R-trz ligands: *i*. *N*-salicylidine-4-amino-1,2,4-triazole (saltrz), *ii*. 4-(*o*-nitrobenzyl)imino-1,2,4-triazole (o-Ntrz), *iii*. 4-phenylimino-1,2,4-triazole (bztrz), *iv*. 2,5-dichloride-4-phenylimino-1,2,4-triazole (Cl_2trz), *v*. napthylimino-1,2,4-triazole (napthtrz), *vi*. (E)-N-(furan-2-ylmethylene)-4H-1,2,4-triazol-4-amine (furtrz), *vii*. (E)-*N*-(thiophen-2-ylmethylene)-4*H*-1,2,4-triazole-4-amine (thtrz).

In this report, we focus on dinuclear complexes of the type $[Fe_2(NCX)_4(R\text{-}trz)_5]\cdot$guest (X = S, Se; R-trz = functionalised 1,2,4-triazole ligand; Figure 1a)[8] which act as a basic model of the extensively studied 1-D chain triazole SCO polymers[9] and trinuclear species.[10] This versatile dinuclear unit is comprised of Fe^{II} sites connected *via* short Fe-N-N-Fe bridges arising from three $\mu_{1,2}$-coordinated 1,2,4-triazole ligands. The octahedral Fe^{II} coordination is completed by monodentate 1,2,4-triazole ligands and N-bound chalcogenocyanate anions (i.e., NCS^-, $NCSe^-$), resulting in a neutral dinuclear unit. The particularly facile synthetic aspect of this dinuclear construct is that 1,2,4-triazole ligands are readily functionalised, therefore providing ample opportunity to tailor intra- and inter-molecular interactions and the degree of strain across the short Fe-N-N-Fe bridge. Ligands previously employed in this approach[8] have incorporated hydrogen bonding characteristics, electron withdrawing ability and aromatic character (Figure 1b) and have resulted in dinuclear SCO complexes that display one-step complete and incomplete spin transitions and a range of abrupt and gradual behaviours. We recently reported the first two-step spin transition in this family,[8f] and highlighted its structural and SCO adaptability towards guest molecules. Irrespective of the SCO properties, common to the structures within this growing family are dense networks of supramolecular interactions of the type dinuclear…dinuclear and dinuclear…solvent. This intrinsic feature provides an optimal platform for systematic SCO property assessment and tuning and here we investigate ligand heteroatom substitution effects on spin-state switching and structure.

Results and Discussion

Synthesis and characterisation

Single crystals were prepared by either slow evaporation or ether diffusion reactions. Infrared spectroscopy on all materials show the expected stretching bands for the anions and the R-trz ligands. Elemental (CHN) analysis of the complexes confirm their bulk purity.

$[Fe_2(NCX)_4(furtrz)_5]\cdot furtrz\cdot MeOH$; X = S (furtrz-S) and X = Se (furtrz-Se)

Temperature-dependent magnetic susceptibility measurements (300 – 50 K) were conducted on bulk crystalline samples of **furtrz-S** and **furtrz-Se** covered in a small amount of reaction liquid to avoid solvent loss, which has been observed to diminish, extinguish or vary SCO properties in related dinuclear species.[8c,d] For both **furtrz-S** and **furtrz-Se**, gradual one-step spin transition behaviours are observed (Figure 2). The $\chi_M T$ values above *ca*. 250 K correspond to HS Fe^{II} ions. Below 250 K the $\chi_M T$ values gradually decrease, indicating a HS to LS transition of some of the Fe^{II} sites. For both **furtrz-S** and **furtrz-Se**, the $\chi_M T$ values at 50 K show an approximate 1:1 ratio of HS:LS Fe^{II} sites. The characteristic transition temperatures for **furtrz-S** and **furtrz-Se** are 172 and 205 K, respectively. There is negligible hysteresis in the heating and cooling curves for these materials. The increased transition temperature of **furtrz-Se** compared to **furtrz-S** is consistent with the increased ligand field strength of the $NCSe^-$ anion.

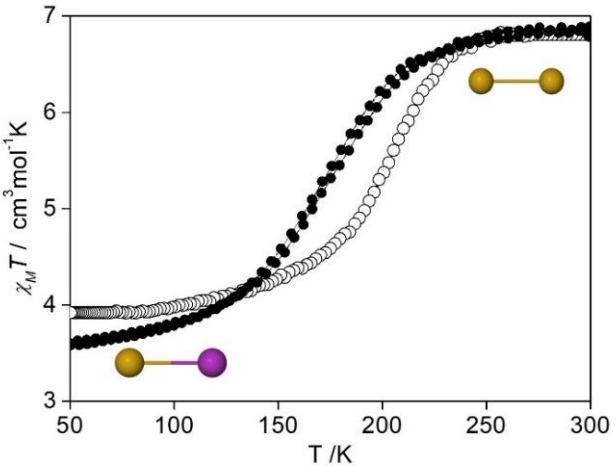

Figure 2. $\chi_M T$ versus temperature per dinuclear for furtrz-S (●) and furtrz-Se (○) over the range 300 – 50 K (scan rate 1 $Kmin^{-1}$). Inset: Schematic of the [Fe1-Fe2] spin state transition from [HS-HS] to [HS-LS] with cooling (HS: yellow, LS: purple).

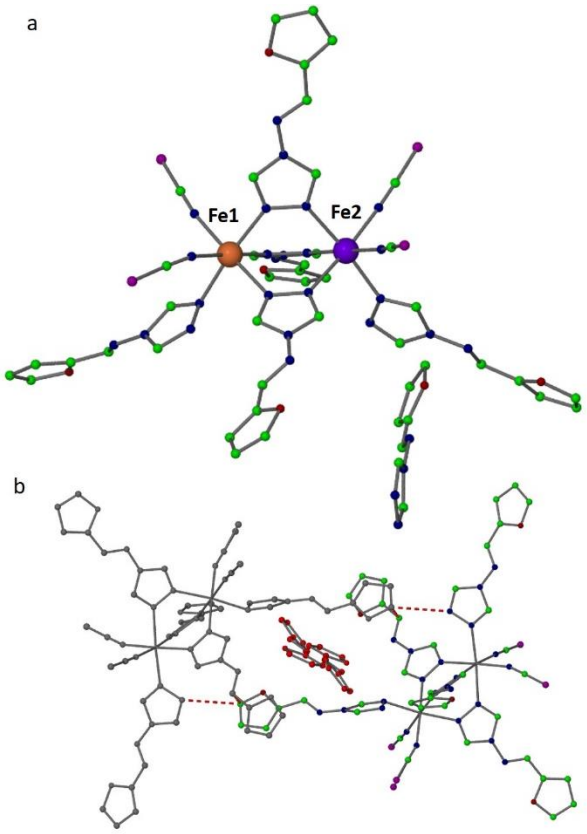

Figure 3. (a) Structural representation of **furtrz-S** at 100 K where the Fe^{II} sites ([**Fe1**-**Fe2**]) within each dinuclear are in the [HS-LS] state. The unbound fur ligand is shown; the guest molecules and hydrogen atoms have been omitted for clarity. (b) Pairs of dinuclear species (shown in grey and colour) with complementary hydrogen-bonding (red dashes) interactions. Unbound fur ligands (red) reside within the dimeric units. Labelling: Fe^{HS} (orange); Fe^{LS} (purple); N (blue); C (green); O (red); S (purple).

Single crystal analyses of **furtrz-S** and **furtrz-Se** were conducted at 100 and 250 K, revealing for both complexes a triclinic symmetry (*P*-1) with an entire dinuclear contained within the asymmetric unit (Figure 3(a)). The complexes **furtrz-S** and **furtrz-Se** are isostructural and remain so independent of changes in temperature and spin-state (Table S1). Each dinuclear unit contains two crystallographically distinct Fe^{II} sites, Fe1 and Fe2 (Figure 3(a); Figure S1-4). Average Fe-N bond length (<$d_{Fe\text{-}N}$>) analysis reveals that for both **furtrz-S** and **furtrz-Se**, Fe1 remains HS and Fe2 transitions to the LS state at 100 K (**furtrz-S**: <$d_{[Fe1,Fe2]\text{-}N}$> /Å 250K = [2.153, 2.189], 100 K = [2.169, 1.995]; **furtrz-Se**: <$d_{[Fe1,Fe2]\text{-}N}$> /Å 250K = [2.136, 2.187], 100 K = [2.162, 1.969]). For both complexes, the degree of octahedral distortion (Σ) at Fe2 decreases over the HS to LS transition as anticipated; however the distortion about Fe1, which remains HS, increases substantially (**furtrz-S**: $\Sigma^{[Fe1,Fe2]}$/°) 250 K = [21.9, 27.9], 100 K = [32.3, 15.1]; **furtrz-Se**: $\Sigma^{[Fe1,Fe2]}$/°) 250 K = [21.9, 29.3], 100 K = [34.1, 20.4]). Enhanced HS distortion concomitant with HS to LS spin transition at a neighbouring site has been previously reported in dinuclear and polymeric complexes and arises from a competition between the HS to LS volumetric contraction, coordination bridges and supramolecular interactions (i.e., competing antiferro- and ferro-elastic interactions).[7] Here, this effect accounts for the trapped [HS-LS] species in both **furtrz-S** and **furtrz-Se** due to effective HS stabilisation at Fe1 across the short and rigid triazole bridge. Such [HS-LS] stabilisation was observed in the related dinuclear $[Fe_2(bztrz)_5(NCS)_2]\cdot x$MeOH (bztrz = 4-phenylimino-1,2,4-triazole).[8d] We also stress that even though the Fe1 centres in the HS species (for both **furtrz-S** and **furtrz-Se**) show significantly shorter average Fe-N bond-lengths, and thus should be more susceptible to undergo SCO than Fe2, they are prevented from doing so by the large angular distortion occurring during SCO.

Alongside the dinuclear moiety (Figure 3(a)), each asymmetric unit contains one unbound fur ligand and one methanol molecule resulting in an overall formula of $[Fe_2(NCX)_4(furtrz)_5]\cdot furtrz\cdot$MeOH for both **furtrz-S** and **furtrz-Se**. The crystal packing is primarily supported by dimeric units of dinuclear species which embrace in mutual hydrogen bonding interactions as depicted in Figure 3(b). The free furtrz ligands reside between these dimeric units and are engaged in dinuclear…ligand hydrogen bonding interactions (Figure S4). Various synthetic attempts were made to prepare dinuclear species without free ligand but without success, suggesting its presence is preferable for efficient solid-state packing. Neighbouring dimeric units are connected *via* secondary hydrogen-bonding interactions (Figure S5). It is likely that the steric effect of the free furtrz ligands in the crystal lattice is a further contributing factor for the incomplete SCO transition and the blocking of the [HS-LS] species at low temperature.

$[Fe_2(NCX)_4(thtrz)_5]\cdot$4MeOH; X = S (thtrz-S) and X = Se (thtrz-Se)

Temperature-dependent magnetic susceptibility measurements (300 – 4 K) were conducted on bulk crystalline samples of **thtrz-S** and **thtrz-Se** covered in a small amount of reaction liquid to avoid solvent loss. For **thtrz-S**, the Fe^{II} sites remain in a HS state to low temperature (Figure 4(a)). Below *ca*. 100 K a rapid decrease in $\chi_M T$ values is seen due to a combination of zero field splitting and weak antiferromagnetic coupling. Using the Van Vleck equation for a pair of S = 2 centres, the theoretical Landé splitting parameter g = 2.00 and the exchange parameter J = -1.35 cm^{-1} were obtained, indicating weak antiferromagnetic coupling between the HS Fe^{II} centres. The zero-field splitting (axial) parameter, D, was not included since we do not have magnetization data to provide any experimental back-up. Because both J and D parameters are strongly correlated and D has been neglected, the estimated J represents the maximum possible value (see Supporting Information). The J and g values obtained are comparable to those reported for analogous dinuclear Fe^{II}-1,2,4-triazole systems.[8]

Magnetic susceptibility measurements (300 – 50 K) on **thtrz-Se** reveal a complete two-step spin transition of the Fe^{II} sites (Figure 4(b)). The $\chi_M T$ values at 250 K are consistent with all of the Fe^{II} sites being in the HS state. With cooling the $\chi_M T$ values decrease between 220 and 110 K with an undulation in $\chi_M T$ values between 185 and 175 K defining a gradual two-step spin transition. The characteristic $T_{½}$ values associated with the two-step SCO are 170 and 200 K. The $\chi_M T$ values at 175 K indicate *ca*.

1:1 ratio of HS:LS Fe^{II} sites. The $\chi_M T$ values below 110 K indicate a near complete conversion of Fe^{II} sites to the LS state. The presence of a SCO transition in **thtrz-Se** compared to the SCO inactivity of **thtrz-S** is likely a result of the greater ligand field strength of the $NCSe^-$ anion.

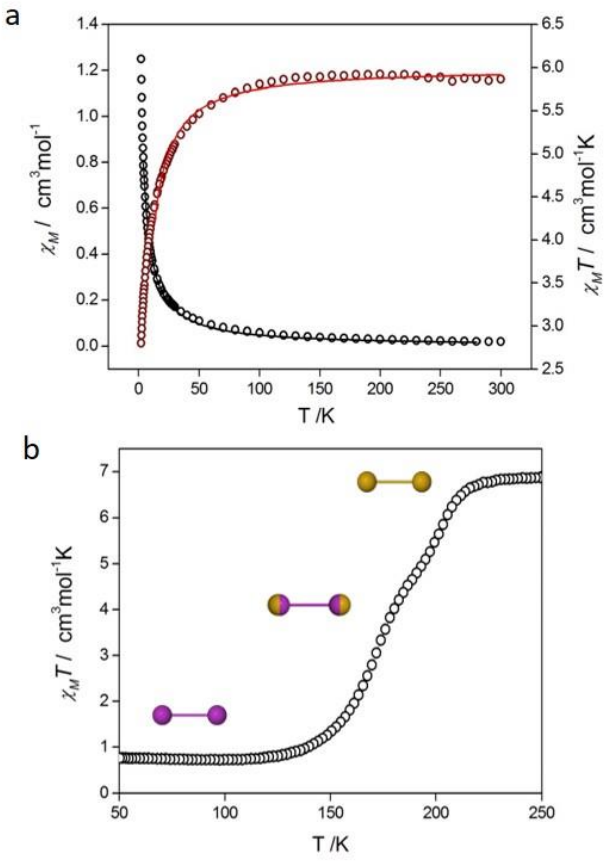

Figure 4: (a) χ_M (○) and $\chi_M T$ (○) versus temperature per dinuclear complex for **thtrz-S** over the range 300 – 4 K; the solid lines represent a least-squares fit to the Van Vleck equation for a pair of $S = 2$ centres. (b) $\chi_M T$ (○) versus temperature per dinuclear complex for **thtrz-Se** over the range 300 – 50 K (scan rate 1 Kmin^{-1}). Inset: Schematic of the [Fe1-Fe1'] spin state transition from [HS-HS'] to [HS/LS-LS'/HS'] to [LS-LS'] with cooling (HS: yellow, LS: purple, yellow/purple: HS/LS disorder).

Despite the distinct magnetic properties, **thtrz-S** and **thtrz-Se** are isostructural, both crystallising in the monoclinic symmetry (space group *C*2/*c*). The asymmetric unit of both contains half a dinuclear complex and thus one crystallographically distinct Fe^{II} site, with the other generated by C_2 axis rotation ([Fe1-Fe1']; Figure 5(a); Table 1). Another consequence of this increased symmetry over that of the furtrz analogues, in which the dinuclear lacks C_2 symmetry, is that one of the thtrz ligands is disordered over two positions over the C_2-axis (Figure 5(a)). Alongside the dinuclear are four methanol molecules, resulting in an overall formula $[Fe_2(NCX)_4(thtrz)_5]\cdot 4MeOH$ for both **thtrz-S** and **thtrz-Se**. For **thtrz-S** the average Fe-N bond length at 100 K is consistent with assignment of HS Fe^{II} ions ($<d_{Fe\text{-}N}>$: 2.154 Å). Quantitative structural analysis of **thtrz-Se**, which was hampered to some degree by partially overlapped twinning (Figure S8; many various synthetic techniques were applied in an attempt to produce monocrystalline sample, but all resulted in intergrown crystals) indicated an isostructural dinuclear moiety to **thtrz-S** (Table S2 and Figure S7). Unit cell analysis was furthermore conducted over the SCO temperature range (Figure S9), revealing a unit cell volume progressing as anticipated for a two-step SCO transition. Importantly, careful structural analysis around the intermediate plateau range (i.e., 185-175 K) revealed the lack of a phase transition. This confirms that at the intermediate plateau there is no 3D long-range ordering of HS and LS sites within each dinuclear unit, a phenomenon which has been observed many times in dinuclear SCO species.[5]

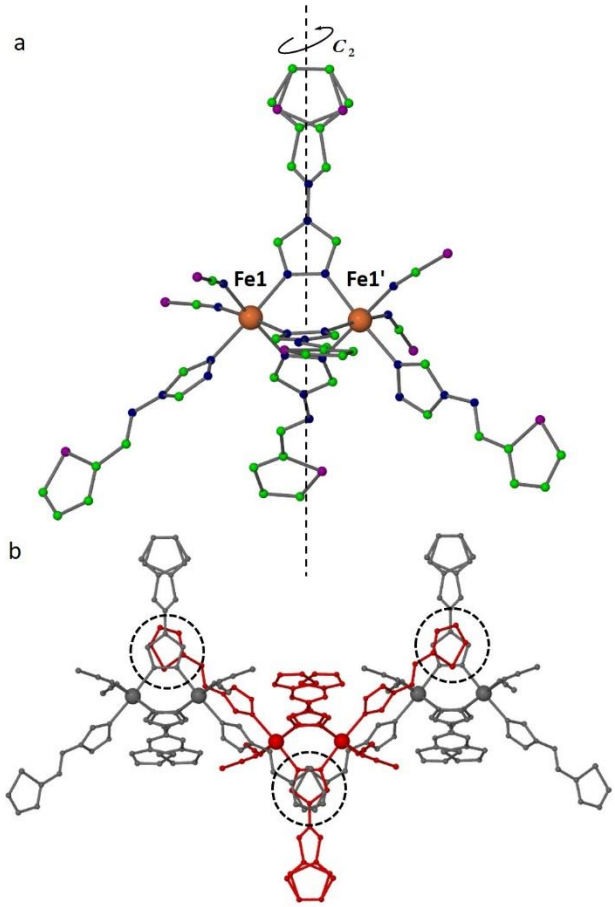

Figure 5. (a) Structural representation of **thtrz-S** at 100 K where the Fe^{II} sites ([Fe1-Fe1']) are in the HS state. Guest molecules and hydrogen atoms have been omitted for clarity. Labelling: Fe^{HS} (orange); N (blue); C (green); O (red); S (purple). (b) Chains of dinuclear species (shown in grey and red for clarity) with regions of π-stacking interactions (indicated by black circles).

Despite the lack of long-range order from a crystallographic perspective, local order within each dinuclear unit exists, most notably as the thiophene ring exists in one of two possible orientations. Indeed, equivalent symmetry, disorder and a two-step SCO transition was observed for the related dinuclear complex $[Fe_2(o\text{-Ntrz})_5(NCS)_4]$ (*o*-Ntrz = 4-(o-nitrobenzyl)imino-1,2,4-triazole).[8f] Therefore, it is likely for **thtrz-Se**, as for $[Fe_2(o\text{-Ntrz})_5(NCS)_4]$, that the local disposition of the disordered functional groups defines a local spin-state ordering (i.e., [HS-LS] and [LS-HS]) and accounts for the presence of a two-step

SCO transition; this effect has been noted previously in other SCO species.[11]

Alongside the dinuclear moiety, each asymmetric unit contains four methanol molecules, resulting in an overall formula of $[Fe_2(NCX)_4(thtrz)_5]\cdot 4MeOH$ for both **thtrz-S** and **thtrz-Se**. As for **furtrz-S** and **furtrz-Se**, and indeed all members of this general class of dinuclear species, the crystal packing is supported by various dinuclear…dinuclear and dinuclear…guest interactions. In particular for **thtrz-S** and **thtrz-Se**, the packing is dominated by chains of π-stacking interactions (see Figure 5(b)). A similar π-stacking interaction array was also observed in $[Fe_2(saltrz)_5(NCS)_4]\cdot 4MeOH$ (saltrz = N-salicylidene-4-amino-1,2,4-triazole), $[Fe_2(o\text{-}Ntrz)_5(NCS)_4]$ and $[Fe_2(o\text{-}Ntrz)_5(NCS)_4]\cdot 3H_2O$.[8b,c,f] Interestingly, of the examples in this growing family of dinuclear species, these and **thtrz-Se** are the only to show either abrupt or two-step SCO transitions. This highlights the communication enhancement role provided by these long-range interactions.

Experimental

General: All reagents were commercially available and used as received (iron(II) perchlorate was handled carefully and in small amounts to avoid any potential explosions).

$[Fe_2(NCS)_4(furtrz)_5]\cdot furtrz\cdot MeOH$ **(furtrz-S):** A methanolic solution (5 mL) of iron(II) perchlorate hexahydrate (34.7 mg, 0.096 mmol), sodium thiocyanate (34.6 mg, 0.427 mmol), ascorbic acid (5 mg) and furtrz (72.2 mg, 0.445 mmol) was slowly evaporated producing block yellow crystals (76.0 mg, 41 %) over a period of 36h. Crystals can also be produced by diethyl ether vapour diffusion into the methanolic solution. Elemental analysis: calcd. C: 40.56, H: 2.62, N: 29.11 exp. C: 40.96, H: 2.86, N: 29.73. IR (cm^{-1}): 3414 (w), 2469 (w), 2358 (m), 2078 (s), 1882 (m), 1584 (s), 1568 (s), 1427 (m), 1387 (m), 1359 (m), 1235 (w), 1197 (w), 1172 (w), 1130 (w), 1061 (w), 1038 (w), 1017 (w).

$[Fe_2(NCSe)_4(furtrz)_5]\cdot furtrz\cdot MeOH$ **(furtrz-Se):** A methanolic solution (5 mL) of iron(II) perchlorate hexahydrate (36.1 mg, 0.099 mmol), sodium selenocyanate (33.4 mg, 0.318 mmol), ascorbic acid (5 mg) and furtrz (79.1 mg, 0.261 mmol) was slowly evaporated producing block yellow crystals (78.2 mg, 35 %) over a period of 36h. Crystals can also be produced by diethyl ether vapour diffusion into the methanolic solution. Elemental analysis: calcd. C: 36.72, H: 2.41, N: 26.07 exp. C: 36.31, H: 2.94, N: 26.33. IR (cm^{-1}): 3278 (w), 3112 (w), 2944 (m), 2831 (w), 2074 (m), 1650 (s).

$[Fe_2(NCS)_4(thtrz)_5]\cdot 4MeOH$ **(thtrz-S):** A methanolic solution (5 mL) of iron(II) perchlorate hexahydrate (33.5 mg, 0.092 mmol), sodium thiocyanate (30.3 mg, 0.374 mmol), ascorbic acid (10-15 mg) and thtrz (79.2 mg, 0.445 mmol) was slowly evaporated producing small yellow crystals (58.3 mg, 33 %) over a period of 36h. Crystals can also be produced by diethyl ether vapour diffusion into the methanolic solution. Elemental analysis: calcd. C: 35.89, H: 3.79, N: 23.42 exp. C: 35.87, H: 3.26, N: 23.85. IR (cm^{-1}): 3372 (w), 3103 (m), 2064 (s), 1591 (m), 1526 (m).

$[Fe_2(NCSe)_4(thtrz)_5]\cdot 4MeOH$ **(thtrz-Se):** A methanolic solution (5 mL) of iron(II) perchlorate hexahydrate (30.1 mg, 0.083 mmol), sodium selenocyanate (33.2 mg, 0.259 mmol), ascorbic acid (10-15 mg) and thtrz (78.2 mg, 0.439 mmol) was slowly evaporated producing small yellow crystals (20.8 mg, 12 %) over a period of 36h. Crystals can also be produced by tert-butylmethyl ether vapour diffusion into the methanolic solution. Elemental analysis: calcd. C: 30.67, H: 3.43, N: 20.44 exp. C: 30.15, H: 3.73, N: 20.27. IR (cm^{-1}): 3372 (w), 3103 (m), 2064 (s), 1591 (m), 1526 (m).

Single crystal X-ray diffraction**:** Single crystal diffraction data were collected on an Agilent Technologies SuperNova Dual Source diffractometer using either a Cu-K_α (λ = 1.54184 Å) or Mo-K_α (λ = 0.71073 Å) radiation source using an Oxford Cryostreams Cryostream attachment. Crystals were mounted on MiTeGen loops using paratone-N oil. Full spheres of data were collected over a range of incident angles. Data integration and reduction were performed using CrysAlisPro SuperNova software.[12] The structures of all materials was solved within SHELXT and refined using SHELXL within the X-SEED user interface.[13] Solvent molecules were located on a difference Fourier map and hydrogen atoms were placed in geometrically idealised positions and fixed using the riding model. All atoms were refined anisotropically unless otherwise stated. Crystallographic refinement details are presented in Tables S1-3 and ORTEP diagrams in Figures S1-4 and S7. The CCDC reference numbers are 1884823-1884827 for **furtrz-S** (250 K), **furtrz-Se** (250 K), **thtrz-S** (100 K), **furtrz-Se** (100 K), **furtrz-S** (100 K), respectively.

Magnetic Susceptibility**:** Temperature dependent magnetic susceptibility data were collected using either a Quantum Design Versalab with vibrating sample magnetometer (VSM; field of 0.3 T; sweep mode with no overshoot; 300 - 50 K; scan rate 1 $Kmin^{-1}$) or a Quantum Design PPMS magnetometer (field of 1 T; settle mode; 300 - 4 K). Polycrystalline samples were loaded into polypropylene sample holders (Formolene® 4100N), which were sealed with Teflon tape to prevent solvent loss. For measurement, the sample holders were enclosed in a brass half-tube.

Conclusions

In summary, we present four new molecular materials of the type $[Fe^{II}_2(R\text{-}trz)_5(NCX)_4]\cdot guest$ (R-trz = furtrz, thtrz; X = S, Se) with heteroatom substituted functional groups. We show that the flexible network of supramolecular interactions intrinsic to this class of dinuclear species drives a broad array of ligand and crystal-packing sensitive spin-state switching properties, including the presence of an elastically frustrated 'blocked' [HS-LS] species and a rare two-step SCO transition.

Within the furan-appended ligand family (**furtrz-S** and **furtrz-Se**) the structures are dominated by dimers of interacting dinuclear units and gradual one-step SCO transitions prevail. In contrast, while within the thiophene-appended ligand family the NCS^- analogue (**thtrz-S**) is SCO-inactive (HS), the $NCSe^-$ analogue displays a rare two-step SCO transition. While the reason for the SCO-inactivity of **thtrz-S** is unclear, a clear distinction between this and the furan-family is that the crystal packing is dominated by 1-D arrays of π-stacking interactions. This type of supramolecular interaction network would undoubtedly provide superior solid-state communication pathways as was seen in several related dinuclear species.[8b,c,f]

With respect to the emergence of a two-step SCO transition in **thtrz-Se**, the presence of one crystallographically distinct Fe^{II} site per dinuclear (due to the presence of a C_2 axis) is perhaps counterintuitive, but has been observed previously within this dinuclear family.[8b,f] We rationalise this as locally the Fe^{II} sites have slightly different environments due to two-fold ligand disorder therefore resulting in a two-step transition (potentially with partially cooperative or anti-cooperative intramolecular interaction between sites). Intermolecular cooperativity then makes the transition sufficiently sharp such that the two-step transition is apparent rather than a gradual one-step transition. Amongst discrete SCO materials, dinuclear species are significant as they represent a basic prototype of a polymeric

species. Thus, from a fundamental perspective, this study offers further insight into cooperative effects of coordination links between SCO sites in dinuclear species. Overall, our detailed structural analyses show that the major difference between these and other reported dinuclear species in this family is in the complexity and effectiveness of the supramolecular interaction pathways. Collectively, of the functionalised 1,2,4-triazole ligands thus far studied in this general class of dinuclear species, the ones with direct hydrogen bonding capacity (i.e., -OH and -NO_2)[8b,f] have produced by far the most abrupt spin transitions, indicating that supramolecular interactions are intrinsic to effect communication in this family. Finally, this study highlights how subtle variation in supramolecular interaction pathways largely modulate spin-state switching cooperativity profiles.

Acknowledgements

The Australian Research Council is thanked for providing Discovery Project Grants and a Future Fellowship to support this collaborative work at the University of Sydney and UNSW Sydney. We also acknowledge the University of Basel for support and funding from the UK EPSRC grant EP/K013009/1.

References

1 (a) O. Kahn, M. C. Jay, *Science*, 1998, **279**, 44–48; (b) P. Gütlich, H. A. Goodwin, *Top. Curr. Chem.* 2004, **233-235**; (c) M. A. Halcrow, Spin-crossover materials: properties and applications, John Wiley & Sons, 2013; (d) K. S. Kumar, M. Ruben, *Coord. Chem. Rev.* 2017, **346**, 176-205.

2 M. A. Halcrow, *Chem. Soc. Rev.* 2011, **40**, 4119-4142.

3 N. Willenbacher, H. Spiering, *J. Phys. C Solid State Phys.*, 1988, **21**, 1423–1439.

4 K. S. Murray, C. J. Kepert, *Top. Curr. Chem.*, 2004, **233**; R. W. Hogue, S. Singh, S. Brooker, *Chem. Soc. Rev.* 2018, **47**, 7303.

5 (a) J. A. Real, H. Bolvin, A. Bousseksou, A. Dworkin, O. Kahn, F. Varret, J. Zarembowitch, *J. Am. Chem. Soc.* 1992, **114**, 4650-4658; (b) N. O. Moussa, G. Molńar, S. Bonhommeau, A. Zwick, S. Mouri, K. Tanaka, J. A. Real, A. Bousseksou, *Phys. Rev. Lett.*, 2005, **94**, 107205; (c) E. Trzop, M. B. Cointe, H. Cailleau, L. Toupet, G. Molńar, A. Bousseksou, A. B. Gaspar, J. A. Real, E. Collet, *J. App. Cryst.*, 2007, **40**, 1, 158-164; (d) A. B. Gaspar, M. C. Muñoz, J. A. Real, *J. Mater. Chem.*, 2006, **16**, 2522-2533, (e) J. Olguín, S. Brooker, Spin-crossover in discrete polynuclear complexes in Spin-Crossover Materials: Properties and Applications, John Wiley & Sons, Ltd. Chichester, UK, 2013, 77.

6 K. Nakano, S. Kawata, K. Yoneda, A. Fuyuhiro, T. Yagi, S. Nasu, S. Morimoto, S. Kaizaki, *Chem. Comm.* 2004, 2892-2893.

7 M. Paez-Espejo, M. Sy, K. Boukheddaden, *J. Am. Chem. Soc.*, 2016, **138**, 3202–3210; N. F. Sciortino, K. A. Zenere, M. E. Corrigan, G. J. Halder, G. Chastanet, J.-F. Létard, C. J. Kepert, S. M. Neville, *Chem. Sci.* 2017, **8**, 701-707.

8 (a) J. J. A. Kolnaar, M. L. de Heer, H. Kooijman, A. L. Spek, G. Schmitt, V. Ksenofontov, P. Gütlich, J. G. Haasnoot, J. Reedijk, *Eur. J. Inorg. Chem.* 1999, **5**, 881-886; (b) Y. Garcia, F. Robert, A. D. Naik, G. Zhou, B. Tinant, K. Robeyns, S. Michotte, L. Piraux, *J. Am. Chem. Soc.* 2011, **133**, 15850-15853; (c) H. A. Scott, T. M. Ross, B. Moubaraki, K. S. Murray, S. M. Neville, *Eur. J. Inorg. Chem.* 2013, 803-812; (d) O. Roubeau, R. Gamez, S. J. Teat, *Eur. J. Inorg. Chem.* 2013, 934-942; (e) X. Cheng, Q. Yang, C. Gao, B.-W. Wang, T. Shiga, H. Oshio, Z.-M. Wang, S. Gao, *Dalton Trans*. 2015, **44**, 11282-11285; (f) J. E. Clements, P. R. Airey, F. Ragon, V. Shang, C. J. Kepert, S. M. Neville, 2018, **57**, 17, 11068-11076.

9 (a) J. G. Haasnoot, *Coord. Chem. Rev.* 2000, **131**(200–202), 131-185; (b) O. Roubeau, *Chem. Eur. J.* 2012, **18**, 15230-15244; (c) A. Grosjean, P. Négrier, P. Bordet, C. Etrillard, D. Mondieig, S. Pechev, E. Lebraud, J.-F. Létard, P. Guionneau, P. *Eur. J. Inorg. Chem.* 2013, **5-6**, 796-802; (d) M. B. Bushuev, D. P. Pishchur, I. V. Korolkov, K. A. Vinogradova, *Phys. Chem. Chem. Phys.* 2017, 4056-4068.

10 (a) Y. Garcia, P. Guionneau, G. Bravic, D. Chasseau, J. A. K. Howard, O. Kahn, V. Ksenofontov, S. Reiman, P. Gütlich, *Eur. J. Inorg. Chem.* 2000, 1531-1538; (b) V. Gómez, J. Benet-Buchholz, E. Martin, J. R. Galán-Mascarós, *Chem. Eur. J.* 2014, **20**(18), 5369-5379; (c) N. Pittala, F. Thétiot, C. Charles, S. Triki, S. Boukheddaden, G. Chastanet, M. Marchivie, *Chem. Comm.* 2017, **53**(59), 8356-8359.

11 (a) B. Weber, C. Carbonera, C. Desplances, J.-F. Létard, *Eur. J. Inorg. Chem.* 2008, 1589-1598; (b) S. Schlamp, B. Weber, A. D. Naik, Y. Garcia, *Chem. Comm.* 2011, **47**, 7152-7154; (c) W. Bauer, M. M. Dîrtu, Y. Garcia, B. Weber, *Cryst. Eng. Comm.* 2012, **14**, 1223-1231;

12 CrysAlisPro 2013, Agilent Technologies V1.171.36.28.

13 L. J. Barbour, X-SEED, University of Stellenbosch, South Africa, 1999.

